Available online at www.sciencedirect.com
SCIENCE DIRECT®
Journal of Chromatography A, 1021 (2003) 201–207
JOURNAL OF CHROMATOGRAPHY A
www.elsevier.com/locate/chroma

Subsecond separation of cellular flavin coenzymes by microchip capillary electrophoresis with laser-induced fluorescence detection

Bi-Feng Liu*, Hideaki Hisamoto, Shigeru Terabe

Graduate School of Science, Himeji Institute of Technology, Kamigori, Hyogo 678-1297, Japan

Received 2 June 2003; received in revised form 4 September 2003; accepted 4 September 2003

Abstract

In this article, it was demonstrated that a subsecond separation of cellular metabolites such as riboflavin (RF), flavin mononucleotide (FMN), and flavin–adenine dinucleotide (FAD) was achieved using microchip capillary electrophoresis with laser-induced fluorescence detection. The influences of crucial parameters that governed analysis time (e.g., channel length and electric field for separation) and separation resolution (e.g., sample size) were investigated, both in theoretical aspects and experimental practice. Quantitative analyses were performed that exhibited linear dynamic range of two orders of magnitude, with calculated detection limits of 34, 201, and 127 nM for RF, FAD, and FMN, respectively. To test the validity of the method, it was successfully applied to characterize several recombinant flavin-binding domains in a human neuronal nitric oxide synthase.

Keywords: Subsecond separations; Chip technology; Flavin coenzymes; Riboflavin; Flavin mononucleotide; Flavin–adenine dinucleotide

1. Introduction

Currently, a rapidly increasing interest in microchip-based capillary electrophoresis (μCE) as a new concept platform for analysis is highly focused [1–5]. Advances in many aspects of μCE, for example, injection [6–9], separation [10–16], detection [3,17–22], and signal process [19,23,24] as well as integrated on-chip sample preparation [25] and reaction [8,26] have been dramatically achieved. As a downscaling format of conventional capillary electrophoresis (CE), it naturally inherits and further enhances these advantages of CE such as high-performance separation ability and low sample/reagent consumption. Moreover, integration capability makes it very convenient to perform complicated tasks. Consequently μCE has been recognized as a powerful tool in a wide range of chemical and biochemical analyses [27–29].

μCE separations are usually accomplished in seconds. Compared with the time cost of CE in minutes and liquid chromatography in more than an hour, such a speed is already very rapid. However, to fulfill the requirements of emerging research areas, subsecond speed represents a new challenge for μCE, which is particularly vital for high-throughput screening (HTS) and multidimensional profiling of complex systems. The importance of high-speed analysis to HTS is self-evident: it can remarkably increase the information output per unit time. As for the latter case, for instance, to achieve a two-dimensional separation on a microchip, the sampling rate from the first dimension to the second is absolutely dependent on the separation speed in the second dimension. However, little attention has been paid to subsecond separation area [30]. The concept of subsecond separation can be actually dated back to a decade ago when Moore and Jorgenson [31] introduced an optically gated injection (OGI) to conventional CE for zone broadening study. Four fluorescently tagged amino acids were well separated less than 1 s. The configuration of OGI was afterwards adapted by other researchers for subsecond level analysis [32] or photochemical dynamics monitoring [33]. Almost at the same time, Ramsey's group achieved a subsecond separation [34] and later a submilisecond-speed separation [35] by μCE, which revealed great potentials for ultra high-speed separation. Soon thereafter, such methodology was delicately adopted for a two-dimensional separation system on a microchip by the same group [36]. More recently, Plenert and Shear [37] proposed a microsecond elec-

* Corresponding author. Tel.: +81-791-58-0171; fax: +81-791-58-0493.
E-mail address: bf_liu@sci.himeji-tech.ac.jp (B.-F. Liu).

0021-9673/$ – see front matter © 2003 Elsevier B.V. All rights reserved.
doi:10.1016/j.chroma.2003.09.012

trophoretic separation of two biogenic amines, which paved an avenue to probe reaction intermediates or other transient species.

In this article, subsecond separation of cellular flavin coenzymes was demonstrated using μCE coupled with laser-induced fluorescence (LIF) detection. To achieve such a purpose, the length of channel and the electric field for separation, as well as the sample injection, were investigated. Emphasis was placed on the modulation of sample size that proved to be crucial both from theory consideration and in experimental practice. The established method was successfully applied to characterize the recombinant electron transfer proteins, which was, to our best knowledge, the first report of real-world application by subsecond separation.

2. Experimental

2.1. Chemicals

Flavins including riboflavin (RF), flavin mononucleotide (FMN), and flavin–adenine dinucleotide (FAD) as shown in Fig. 1, were purchased from Wako (Tokyo, Japan), Sigma Chemical Co. (St. Louis, MO, USA), and TCI Chemicals (Tokyo, Japan), respectively. Because the flavins were sensitive to light, their stock solution (8×10^{-4} M for RF, 1×10^{-2} M for FMN and FAD) were prepared in amber glass bottles with pure water, and then stored at 4 °C. Aliquots were then diluted with running buffer as needed. Phosphate-buffered saline (PBS) solution was used as the electrophoretic buffer at pH 8.0, 9.0, and 10.0, and filtered through a 0.45 μm membrane prior to use. All the chemicals were of analytical grade. Water used for all the solutions preparation was purified by a Milli-Q system (Millipore, Bedford, MA, USA).

2.2. Instruments and procedures

Analyses were carried out on a laboratory-built μCE–LIF system that was constructed on an inverted fluorescence microscope (IX70, Olympus, Japan). An argon-ion laser (Spectra-Physics) emitting a blue line at 488 nm was introduced into the microscope. The laser beam was first filtered through a 460–490 nm band-pass filter, reflected by a 510 nm dichroic mirror, and then focused to the microchannel by a 20× objective. Fluorescence was collected by the same objective, filtered through a 515 nm high-pass filter, and finally detected by a charge-coupled device (CCD) camera (model PMA-11, Hamamatsu Photonics). Power supply (Matsusada Precision Devices) for μCE was computer-controlled with terminal emulation software KTX (freeware) connected to a D/A converter (Nippon Filcon, Inagi, Japan) via an RS-232C serial interface.

The glass microchip with a channel pattern of a cross employed in this study, was a gift from Kitamori group (University of Tokyo, Japan). The microchip was fabricated using standard photolithographic, wet chemical etching, and bonding techniques as previously described in [38]. The channel was 80 μm in width on the top and 40 μm in depth. For new microchip, channels were washed sequentially with methanol, water, 1 M NaOH, 0.1 M HCl, 0.1 M NaOH, water and running buffer at room temperature. Between runs, channels were rinsed in an order of 0.1 M NaOH, water and running buffer to ensure the separation reproducibility.

3. Results and discussion

When trying subsecond separation by μCE, two major considerations are naturally involved at the first glance of this topic: how to control the analysis time within 1 s and how to resolve all interest analytes in such short time. It seems easy to achieve the first issue by simply shortening

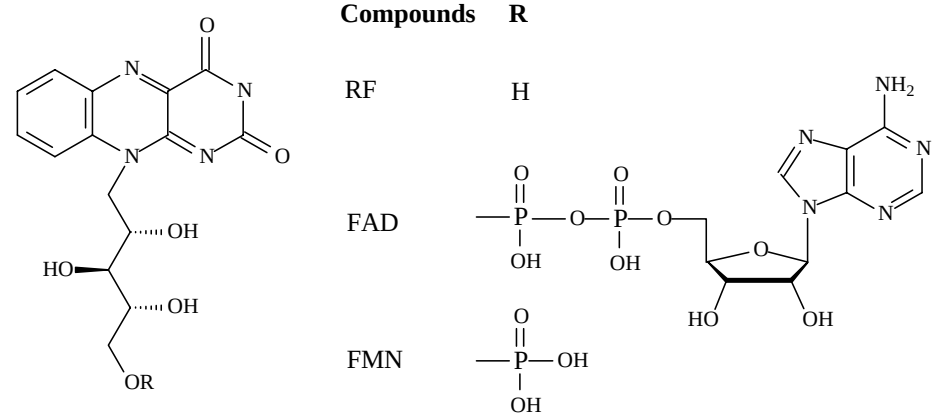

Fig. 1. Molecular structure of flavin metabolites.

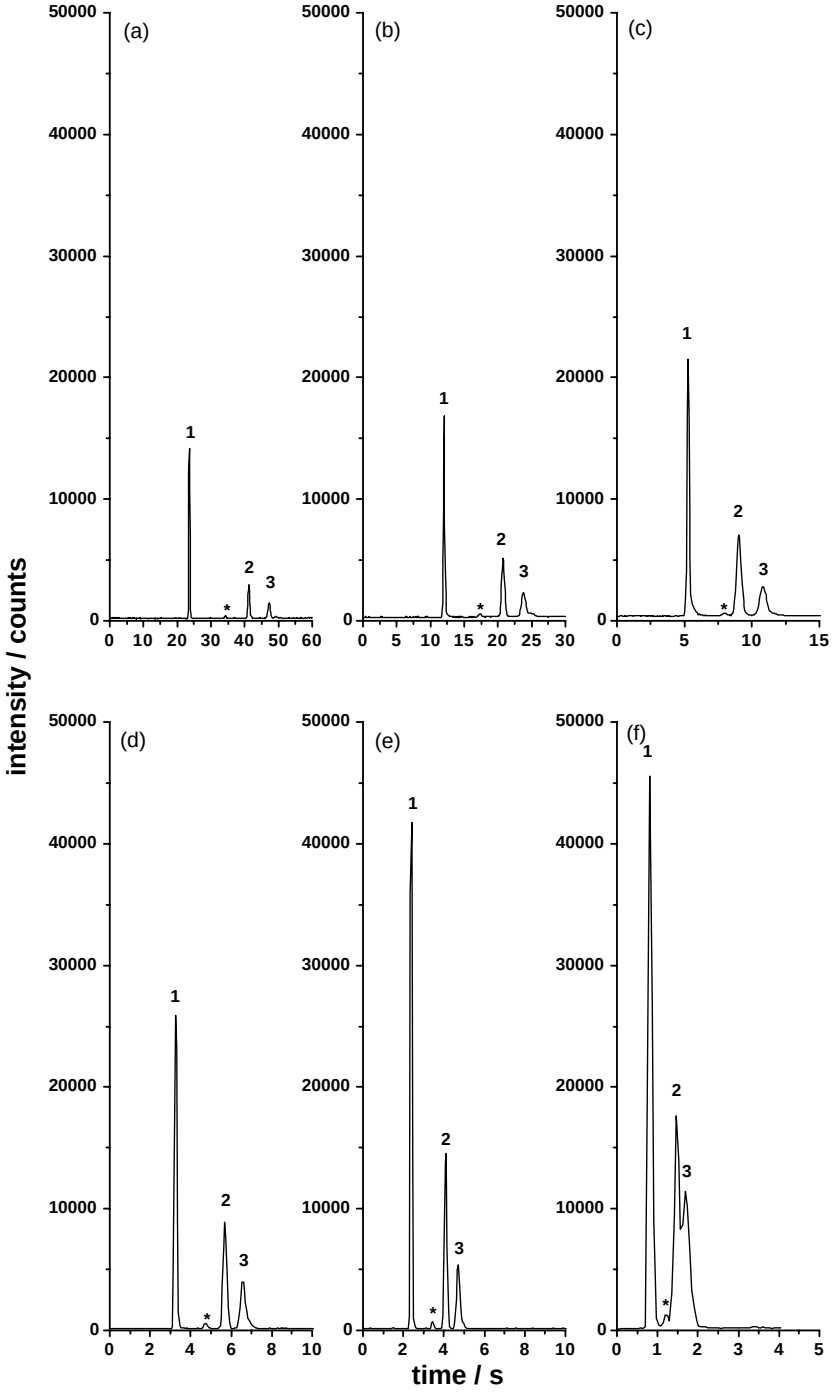

Fig. 2. Electropherograms by μCE–LIF with gated injection mode (300 V cm^{-1} for 0.1 s). Peak identity: (1) RF (4.0 μM); (2) FAD (10.0 μM); (3) FMN (10.0 μM); and (*) impurity. Separation conditions: buffer, 40 mM PBS (pH 9.0); (a) length to the detector (L_d) = 30 mm, E = 300 V cm^{-1}; (b) L_d = 15 mm, E = 300 V cm^{-1}; (c) L_d = 5 mm, E = 300 V cm^{-1}; (d) L_d = 5 mm, E = 400 V cm^{-1}; (e) L_d = 5 mm, E = 500 V cm^{-1}; and (f) L_d = 2 mm, E = 500 V cm^{-1}.

the separation length (L_{sep}) or increasing the electric field (E) [39] In an extreme case [37], for instance, the values of L_{sep} and E have been adjusted to 9 μm and 0.15 MV cm^{-1}, respectively, to achieve an analysis time of 10 μs. For the second issue, there are various approaches in μCE to finely tune the selectivity of different analytes according to their intrinsic characteristics. However, discussions on specific strategy only functions within certain kind of chemicals, and is not in universal. Therefore, we alternatively consider and evaluate it in a more general and feasible way, the peak capacity (n) that is defined as total number of peaks that can be accommodated at a specific resolution (R_s) over the migration length (L) that distributes zones as follows [40]:

$$n = \frac{L}{[4\sigma R_s]} \quad (1)$$

R_s in Eq. (1) totally depends on analytical goal, thereby it is no meaning for enhancing n. The most crucial factor that effectively influences the peak capacity is peak standard deviation (σ) or peak variance (σ^2). Consequently we investigated σ^2 instead of n for further optimizing our subsecond separations. Assuming that the contributions to σ^2 from adsorption, Joule-heating, electrodispersion, and response time constant of detector can be negligible, the total variance can be written in a sum of variances due to longitudinal diffusion (σ^2_{dif}), injection (σ^2_{inj}) and detection (σ^2_{det}) as follows:

$$\sigma^2 = \sigma^2_{dif} + \sigma^2_{inj} + \sigma^2_{det} \quad (2)$$

The zone spreading by longitudinal diffusion can be described by Einstein's equation. Since the sample plug injected into the separation channel is considered as a bell shape that can be fitted into a Gaussian function, and the detection path is a rectangular window, the variance from the injection, and the detection can be estimated by theoretically calculating the second central statistic moment of the shape function. Thus, Eq. (2) can be extended to:

$$\sigma^2 = 2Dt + \frac{l^2_{inj}}{16} + \frac{l^2_{det}}{12} \quad (3)$$

where D, l_{inj}, and l_{det} represent the diffusion coefficient of the analyte, baseline width of sample plug, and the window size for detection, respectively. In conventional CE, the contributions to the total peak variance from injection and detection can be neglected because their values are too small compared with that from diffusion. However, it is not the case for very fast separation like subsecond separation in this work, since band broadening by longitudinal diffusion in very short time can be comparable with that by injection and detection. Taking a small molecule rhodamine B as an example, its diffusion coefficient was measured to be $3 \times 10^{-6}\,cm^2\,s^{-1}$. In 1 s, the variance from diffusion will be $6 \times 10^{-6}\,cm^2$. Using the channel width (80 μm) of the microchip as the baseline width of injection plug, we can easily obtain the variance of injection contribution, that is, $4 \times 10^{-6}\,cm^2$. It is indicated by Eq. (3) that the peak variance can be effectively minimized through controlling analysis time, sample plug, and detection window size. In the practice of this study, an analysis time of maximum 1 s is our goal, and the detection window size is an instrument parameter. Thus, both of them are pre-determined. As a consequence, to adjust the sample size is the right way to gain a better peak capacity. Certainly, the detection window size can be also modulated by spatial confinement to the detector that is necessary in case of ultra-fast separation at a time scale of submilisecond. But remember that it will decrease the detection sensitivity at the same time.

Based on above discussion in theory, subsecond separation and determination of cellular flavin metabolites namely RF, FAD, and FMN were studied accordingly. Fig. 2 described a series of electropherograms by μCE with gated injection mode (300 V cm^{-1} for 0.1 s). Besides the three analytes, a contaminant in sample was also included in the electropherograms marked by an asterisk. As shown in Fig. 2a–c, the analysis time was shortened accordingly with the decrease of separation length from 30 to 5 mm. Fig. 2c–e depicted a trend that the analysis time was further decreased by enhancing electric field from 300 to 500 V cm^{-1}. It was not surprising that the peak heights of all analytes increased due to less sample diffusion. In Fig. 2e, a good separation of four components was illustrated in 5 s. On the route of reducing the time for analysis from Fig. 2a–e, no problem on the selectivity occurred. Unfortunately, The peaks of FAD, FMN, and the contaminant were overlapped as shown in Fig. 2f, when continuing to reduce the separation length to 2 mm for further shortening the analysis time. So, the sample size should be reduced to improve the separating resolution. In gated injection mode for μCE, the sample size was linearly related to injection time. As a result, decreasing the injection time would accordingly reduce the sample size. However, our μCE–LIF adopted a multiple power supply system without any relay. The gated injection was achieved by potentials change in each reservoir, not by floating at the buffer reservoir through a relay control. Because of the existence of the ramp time of high voltage supply, the reproducibility of injections below 0.1 s became poor. So, we focused our attention to pinched injection mode, by which the sample size could be well defined [41], by sample pinching factor (p) and sample dispensing factor (d).

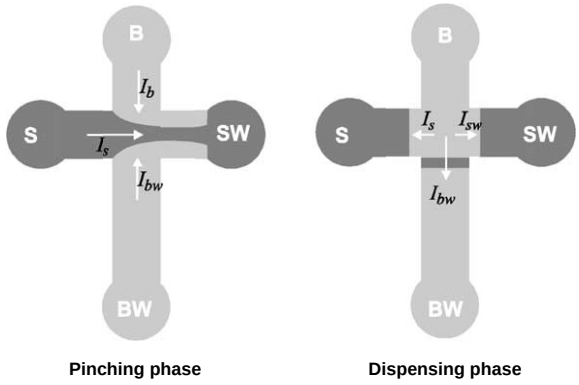

Fig. 3. Schematic description of pinched injection mode for μCE–LIF.

Fig. 3 briefly introduced the strategy of pinched injection mode. When the sample was loaded from sample reservoir (S) to sample waster reservoir (SW), it was pinched at the cross section by streams from buffer reservoir (B) and buffer waste reservoir (BW). The pinching factor p was defined as follows:

$$p = \frac{I_b}{I_s} \quad (4)$$

where I_b and I_s represent currents in buffer and sample channels, providing that the sample stream was symmetrically

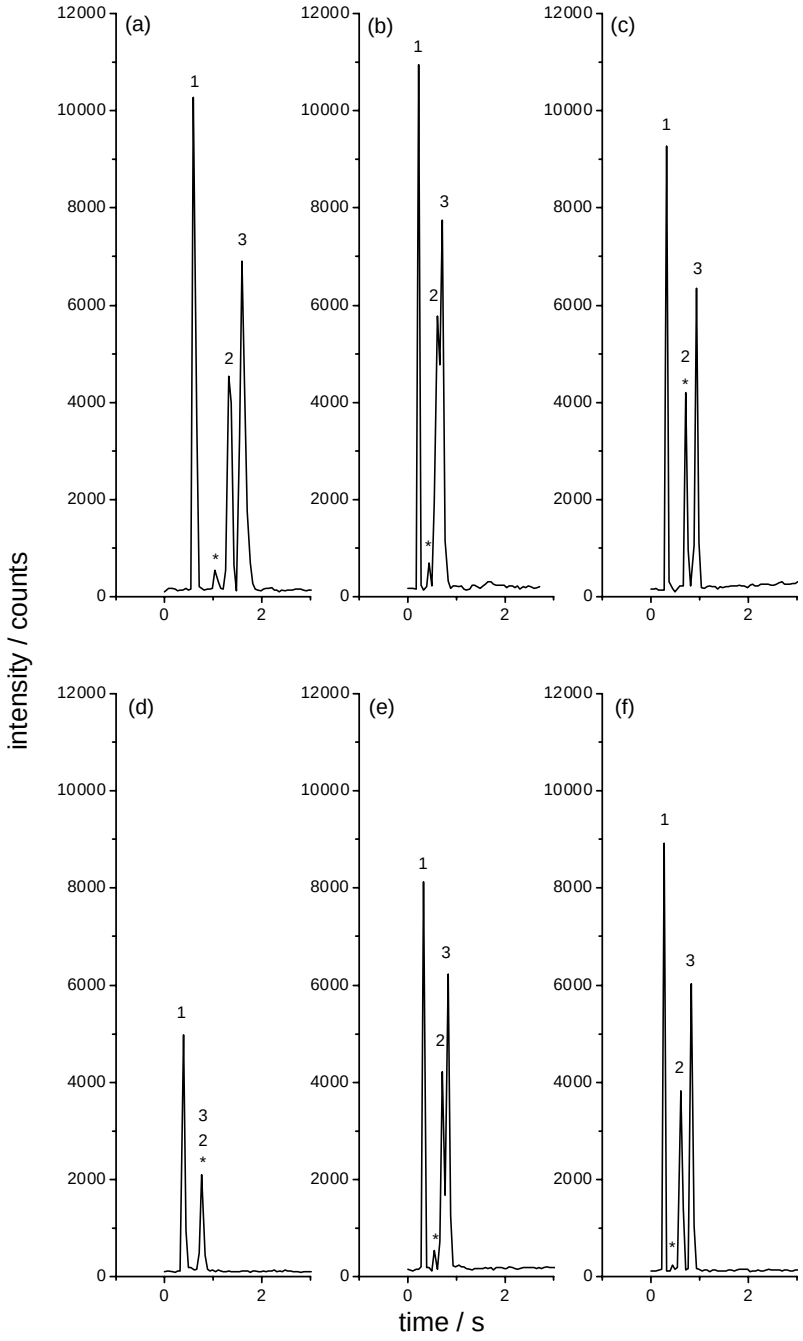

Fig. 4. Electropherograms by μCE–LIF with pinched injection mode. Peak identity: (1) RF (4.0 μM); (2) FAD (10.0 μM); (3) FMN (10.0 μM); and (*) impurity. Separation conditions: (a) buffer: 40 mM PBS (pH 9.0), $E = 500\,\mathrm{V\,cm^{-1}}$, p and $d = 1.5$; (b) buffer: 40 mM PBS (pH 9.0), $E = 700\,\mathrm{V\,cm^{-1}}$, p and $d = 1.5$; (c) buffer: 20 mM PBS (pH 9.0), $E = 700\,\mathrm{V\,cm^{-1}}$, $p = 2.0$ and $d = 1.5$; (d) buffer: 20 mM PBS (pH 10.0), $E = 700\,\mathrm{V\,cm^{-1}}$, $p = 2.0$ and $d = 1.5$; (e) buffer: 20 mM PBS (pH 8.0), $E = 700\,\mathrm{V\,cm^{-1}}$, $p = 2.0$ and $d = 1.5$; and (f) buffer: 20 mM PBS (pH 9.0), $E = 700\,\mathrm{V\,cm^{-1}}$, $p = 2.0$ and $d = 1.0$.

pinched ($I_b = I_{bw}$). Values for p of >1, =1, and <1 correspondingly represent a strong, moderate, and weak pinching. The well-defined sample plug at the cross section was then dispensed into separation channel for analysis. The percentage of injected portion was determined by dispensing factor d as follows:

$$d = \frac{I_{bw}}{I_s} \tag{5}$$

supposing that the samples dispensed into sample and sample waste channel were identical ($I_s = I_{sw}$). Values for d of >1, =1, and <1 represent a strong, moderate, and weak dispensing, respectively. So, the sample size for separation was actually determined by the two factors p and d. Fig. 4a gave an electropherogram with pinched injection mode (p and $d = 1.5$). Other condition were the same as in Fig. 2f. The four components were well resolved in 2 s.

Table 1
Quantitation information for three metabolites

Compound	Calibration curve	γ	Linear range (μM)	Detection limit (nM)
RF	$y = 2183.1x + 96.5$	0.9989	0.10–10.0	34
FAD	$y = 308.8x + 19.4$	0.9966	0.50–50.0	201
FMN	$y = 596.7x + 14.2$	0.9981	0.50–50.0	127

y: peak height (counts); and x: sample concentration (μM).

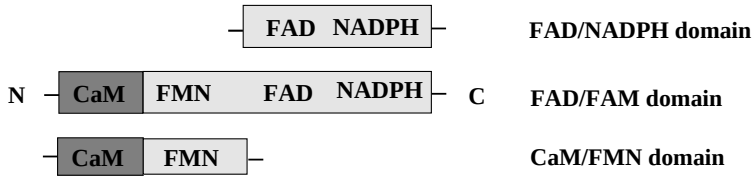

Fig. 5. Structure of recombinant domains of electron transfer protein nNOS.

The change of relative heights of peaks indicated a difference between the two injection strategies, comparing Fig. 4a with Fig. 2f. Further attempt to control the analysis time within 1 s was conducted as shown in Fig. 4b by promoting the separation electric field to 700 V cm^{-1}. However, the peaks of FAD and DMN were overlapped. Changing the pinching factor to 2.0 led to a good resolution for the two peaks as described in Fig. 4c. But the impurity in sample co-eluted with FAD. We tried to adjust buffer pH to improve the separation quality. Unfortunately, neither increasing nor decreasing the buffer acidity could further give any help on improving the resolution as shown in Fig. 4d and e. The much lower peak height in Fig. 4d was mainly caused by influence of buffer acidity on fluorescence characteristics of the analytes. In alkaline solutions, the fluorescent quantum yield of flavin dramatically decreased. So, the dispensing factor was adjusted to 1.0 to reduce the sample dispensed into separation channel. As depicted in Fig. 4f, both subsecond and separation were eventually accomplished.

Quantitative analyses were further carried out on basis of the separation conditions in Fig. 4f. The detection limits for RF, FAD, and FMN were calculated to be 34, 201, and 127 nM, respectively, based on a peak height of three time of the noise. The relative standard deviations (RSDs) were less than 4.0% for migration time and 6.0% for peak height ($n = 7$). Calibration curves, which exhibited a dynamic linear range of 2 orders of magnitude between peak height and concentration of the three metabolites with good correlation coefficients, were established. Relevant quantitative information was summarized in Table 1.

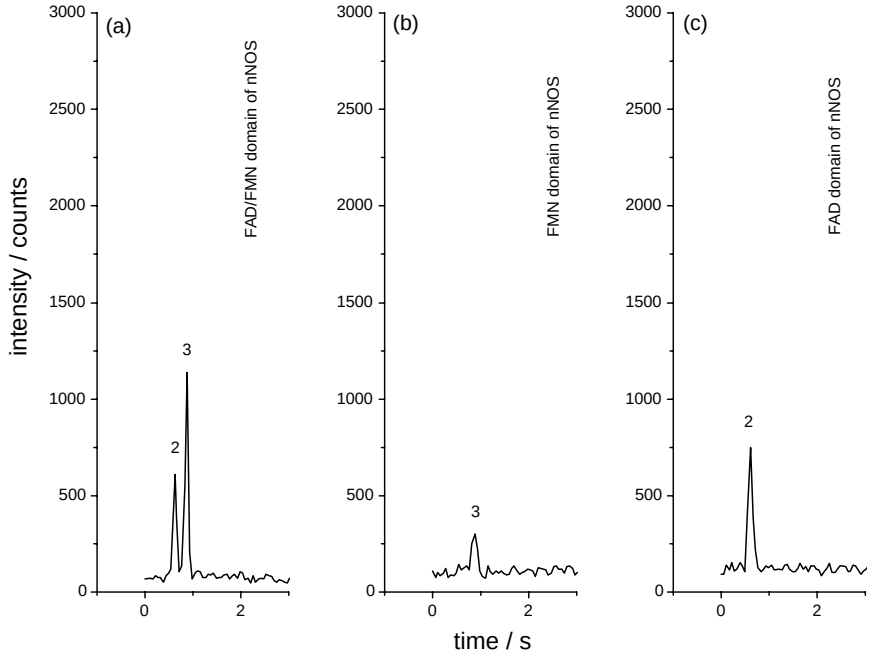

Fig. 6. Electropherograms for characterization of recombinant domains of nNOS by μCE–LIF. Analyses conditions are the same as in Fig. 4; Peak identity: (2) FAD (10.0 μM); (3) FMN (10.0 μM). (a) FAD/FMN domain; (b) FMN domain; (c) FAD domain.

To test the validity of the method, applications to characterize corresponding recombinant domains of a human neuronal nitric oxide synthase (nNOS) [42] were performed under the optimized conditions as in Fig. 4f. Fig. 5 illustrated the structures of constructed domains with particular binding sites. The proteins were harvested from *E. coli* (BL21 line) cells, and then purified. Before the characterization, proteins were heated by a boiling water bath for 10 min, thereby the noncovalently binding FAD or FMN would be released from the proteins. After 15 min centrifugation at 15,000 × *g*, the supernatants were collected and diluted into buffer solution by 10-fold for further μCE analysis. Fig. 6 gave the results. For domains containing one flavin-binding site, sole peak was found in electropherograms (Fig. 6b and c). For the protein containing both FAD and FMN binding sites, a FAD/FMN ratio of 0.92 was revealed (Fig. 6a), which was in good agreement with theoretical expectation of 1/1 molar ratio of FAD/FMN for this flavoenzyme.

4. Conclusion

A subsecond separation of flavin metabolites including RF, FAD, and FMN by μCE–LIF was achieved, with detailed investigations on theoretical aspects and experimental practice. The feasibility of μCE to perform ultra-fast separation was revealed that the separation length and electric field could be conveniently adjusted to shorten analysis time, and the sample size could be controlled to improve the separation quality. Quantitative analyses and applications to characterizing FAD/FMN-binding recombinant proteins proved the reliability of the method, which showed subsecond separation as a promising way to many emerging areas such as HTS and multidimensional profiling of complex systems.

Acknowledgements

The authors gratefully acknowledge the postdoctoral fellowship (to B.-F.L.) and the Grant-in-Aid for Scientific Research (No. P01082) supported by Japan Society for the Promotion of Science (JSPS). Special thanks are given to Dr. Guan and Professor Iyanagi in the Department of Life Science for donating the protein samples.

References

[1] A. Manz, D.J. Harrison, E.M.J. Verpoorte, J.C. Fettinger, A. Paulus, H. Lüdi, H.M. Widmer, J. Chromatogr. 593 (1992) 253.
[2] D.J. Harrison, K. Fluri, K. Seiler, Z. Fan, C.S. Effenhauser, A. Manz, Science 261 (1993) 895.
[3] S.C. Jacobson, R. Hergenröder, L.B. Koutny, J.M. Ramsey, Anal. Chem. 66 (1994) 1114.
[4] D.R. Reyes, D. Iossifidis, P.A. Auroux, A. Manz, Anal. Chem. 74 (2002) 2623.
[5] P.A. Auroux, D. Iossifidis, D.R. Reyes, A. Manz, Anal. Chem. 74 (2002) 2637.
[6] C.S. Effenhauser, A. Manz, H.M. Widmer, Anal. Chem. 65 (1993) 2637.
[7] S.C. Jacobson, R. Hergenröder, L.B. Koutny, R.J. Warmack, J.M. Ramsey, Anal. Chem. 66 (1994) 1107.
[8] S.C. Jacobson, R. Hergenröder, A.W. Moore, J.M. Ramsey, Anal. Chem. 66 (1994) 4127.
[9] D. Solignac, M.A.M. Gijs, Anal. Chem. 75 (2003) 1652.
[10] D.J. Harrison, A. Manz, Z. Fan, H. Lüdi, H.M. Widmer, Anal. Chem. 64 (1992) 1926.
[11] A.W. Moore, S.C. Jacobson, J.M. Ramsey, Anal. Chem. 67 (1995) 4184.
[12] A.T. Wooley, R.A. Mathies, Proc. Natl. Acad. Sci. U.S.A. 91 (1994) 11348.
[13] O. Hofmann, D. Che, K.A. Cruickshank, U.R. Müller, Anal. Chem. 71 (1999) 678.
[14] S.C. Jacobson, R. Hergenröder, L.B. Koutny, J.M. Ramsey, Anal. Chem. 66 (1994) 2369.
[15] N. Burggraf, A. Manz, C.S. Effenhauser, E. Verpoorte, N.F. deRooij, H.M. Widmer, J. High Resolut. Chromatogr. 16 (1993) 594.
[16] D.E. Raymond, A. Manz, H.M. Widmer, Anal. Chem. 66 (1994) 2858.
[17] J. Li, J.F. Kelly, I. Chernushevich, D.J. Harrison, P. Thibault, Anal. Chem. 73 (2001) 599.
[18] P.F. Gavin, A. Ewing, J. Am. Chem. Soc. 118 (1996) 8932.
[19] Y.C. Kwok, N.T. Jeffery, A. Manz, Anal. Chem. 73 (2001) 1748.
[20] A. Arora, J.C.T. Eijkel, W.E. Morf, A. Manz, Anal. Chem. 73 (2001) 3282.
[21] B.-F. Liu, M. Ozaki, Y. Ustumi, T. Hattori, S. Terabe, Anal. Chem. 75 (2003) 36.
[22] K. Uchiyama, A. Hibara, K. Sato, H. Hisamoto, M. Tokeshi, T. Kitamori, Electrophoresis 24 (2003) 179.
[23] K. Hata, Y. Kichise, T. kaneta, T. Imasaka, Anal. Chem. 75 (2003) 1765.
[24] B.-F. Liu, Y. Sera, N. Matsubara, K. Otsuka, S. Terabe, Electrophoresis 24 (2003) 3260.
[25] A.T. Woolley, D. Hadley, P. Landre, A.J. deMello, R.A. Mathies, M.A. Northrup, Anal. Chem. 68 (1996) 4081.
[26] S.C. Jacobson, L.B. Koutny, R. Hergenröder, A.W. Moore, J.M. Ramsey, Anal. Chem. 66 (1994) 3472.
[27] C. S. Effenhauser, in: Microsystem Technology in Chemistry and Life Science, Springer, Berlin, Heidelberg, 1999, p. 51.
[28] V. Dolík, S. Liu, S. Jovanivich, Electrophoresis 21 (2000) 41.
[29] J. Khandurina, A Guttman, J. Chromatogr. A 943 (2002) 159.
[30] R.T. Kennedy, I. German, J.E. Thompson, S.R. Witowski, Chem. Rev. 99 (1999) 3081.
[31] A.W. Moore Jr., J.W. Jorgenson, Anal. Chem. 65 (1993) 3550.
[32] L. Tao, J.E. Thompson, R.T. Kennedy, Anal. Chem. 70 (1998) 4015.
[33] M.J. Gordon, E. Okerberg, M.L. Gostkowski, J.B. Shear, J. Am. Chem. Soc. 123 (2001) 10780.
[34] S.C. Jacobson, R. Hergenröder, L.B. Koutny, J.M. Ramsey, Anal. Chem. 66 (1994) 1114.
[35] S.C. Jacobson, C.T. Culbertson, J.E. Daler, J.M. Ramsey, Anal. Chem. 70 (1998) 3476.
[36] S.C. Jacobson, J.D. Ramsey, C.T. Culbertson, J.M. Ramsey, in: Proceedings of the μTAS 2002 Symposium, p. 608.
[37] M.L. Plenert, J.B. Shear, Proc. Natl. Acad. Sci. U.S.A. 100 (2003) 3853.
[38] A. Hibara, M. Tokeshi, K. Uchiyama, H. Hisamoto, T. Kitamori, Anal. Sci. 17 (2001) 89.
[39] J.W. Jorgenson, K.D. Lukacs, Anal. Chem. 53 (1981) 1298.
[40] J.C. Giddings, Unified Separation Science, Wiley, New York, 1991, p. 105.
[41] J.P. Alarie, S.C. Jacobson, C.T. Culbertson, J.M. Ramsey, Electrophoresis 21 (2000) 100.
[42] Z.W. Guan, T. Iyanagi, Arch. Biochem. Biophys. 412 (2003) 65.